Journal of Statistical Physics, Vol. 63, Nos. 5/6, 1991

The Hard-Sphere Order–Disorder Transition in the Bethe Continuum

A. Robledo[1] **and C. Varea**[1,2]

Received December 12, 1990

We describe a search for solidlike singlet distribution functions in a system of hard spheres. The procedure, which is based on Widom's relation between the activity and the density in a nonuniform fluid, is applied to a sequence of hard-core lattice gases with increasingly extended interactions. When the system is defined on a Bethe lattice we obtain exact solutions for arbitrary external field and size of the hard core. This includes the limit in which the number of excluded neighbors goes to infinity while the lattice spacing is made to vanish. The study of the first few members in this family of models suggests the existence of an infinite sequence, beginning with the next-nearest-neighbor problem, of first-order sublattice ordering transitions occurring before close packing and at zero field. The periodic solutions for the density originate at bifurcation points located at uniform close packing.

KEY WORDS: Hard spheres; ordering transition; density functionals.

1. INTRODUCTION

The study of solidlike states in the hard-sphere fluid system has often taken the form of a search, at high packing fractions, for oscillatory behavior in the equilibrium density, or singlet distribution function $\rho(\mathbf{r})$ (see, e.g., refs. 1 and 2). The framework for these investigations is provided by nonlinear integral equations which relate the density and pair correlation functions of the system.$^{(1,2)}$ These equations always have a uniform liquid density solution, but, because of their nonlinearity, oscillatory solutions may also occur. Provided these solutions appear at the expected mean density of the solid, and with a spatial scale of oscillation compatible with this density,

---

[1] Instituto de Física, Universidad Nacional Autónoma de México, 01000 México, Distrito Federal.

[2] On leave from Facultad de Química, Universidad Nacional Autónoma de México, 04510 México, Distrito Federal.

they may be considered appropriate representations of the solid. According to the general accounts of this approach,$^{(1,2)}$ these calculations have employed one of two such equations: the lowest order integral equation in the BGYB hierarchy, or the Wertheim–Lovett–Mou–Buff (WLMB) integral equation that relates the density to the gradient of the direct pair correlation function $c(\mathbf{r}, \mathbf{r}')$.[3] In all cases, the pair distribution $\rho^{(2)}(\mathbf{r}, \mathbf{r}')$, or the equivalent $c(\mathbf{r}, \mathbf{r}')$, is replaced by its uniform counterpart, typically that predicted by the Percus–Yevick approximation.

An indication that the nonlinear equation method is inconveniently sensitive to approximations is that the work on the BGYB equation finds such oscillatory solutions,$^{(5,6)}$ while that on the WLMB equation does not.$^{(7,8)}$ Moreover, the oscillatory solutions found arise by *bifurcation* off, i.e., continuously out of, the uniform liquid solution, and, as has been pointed out,$^{(8)}$ when this occurs the bifurcation point should also be a state where an instability (in both thermodynamic and mechanical senses) develops. The bifurcation points found for hard disks and spheres within the BYGB scheme are located at otherwise stable liquid states with densities far from close packing, where there is no apparent physical reason for liquid instabilities to occur. Therefore, it has been suggested$^{(2)}$ that these solutions are an artifact of the approximations employed. This view appears reinforced by the encounter, by means of the same method, of a bifurcation point below close packing also in the hard-rod system,$^{(5,6)}$ a system known to exist only in the fluid state. Given this state of affairs, which has remained basically unchanged during the last 10 years, it appears desirable to find a way of performing the nonlinear equation approach, if not to the genuine hard-sphere system itself, to a not-too-trivial model hard-core system without incurring in approximations.

Several years ago$^{(9)}$ Widom's potential-distribution formula$^{(10)}$ was applied to determine expressions for the equation of state of hard-core systems. These expressions take the form of a nonlinear equation relating the density $\rho(\mathbf{r})$ to the activity λ of the system, and constitute an alternative route for the search of solidlike solutions. For one-dimensional hard rods one obtains the exact result of Percus$^{(11)}$ for arbitrary external field, and the bifurcation analysis of this yields *indeed* a branch point at the close-packing density, but the oscillatory solutions remain always confined to this density,$^{(9)}$ and therefore to infinite activity and pressure p, in conformity with the required absence of a phase transition. For the higher-dimensional cases of hard disks and spheres an approximation was proposed,$^{(9)}$ and this yielded bifurcation points at the maximum possible density for the liquid solution, the uniform close-packing density ρ_{ucp}, again a state of infinite λ

---

[3] Independent derivations of this equation appeared first in refs. 3 and 4.

and p (a working definition for ρ_{ucp} is provided below). In these two cases, the oscillatory solutions were found to develop mean densities smaller than ρ_{ucp}, and finite values for λ and p, as they evolved away from the branch point. Presumably, the solidlike solutions, if maintained over a range of densities, may at some state meet the requirements for coexistence with another state belonging to the liquid branch of the free energy. This analysis was not performed, since the approximation was introduced at the level of the equation of state and the free energy density functional was not definable. In all cases, in one and higher dimensions, the branch points were also points of instability with a simple physical interpretation. Hard-core exclusions do not obstruct periodic spatial configurations with wavelength equal to the hard-core size when the uniform system is brought to close packing. There, the response, mechanical or thermodynamic, to external fields that favor spatial density modulations increases without bound. The instability is signaled by the divergence of the structure factor at infinite pressure and activity.

Here we undertake the application of the above technique to hard-core systems defined on the Bethe lattice. Since this would represent an exact model calculation (an example of replacement of the original Hamiltonian by an infinite-dimensional model Hamiltonian), this may provide elements useful in the clarification of some of the issues described, particularly those referring to the occurrence of the instability at close packing and its relation with the order–disorder transition at lower densities.

2. AN INVERSE PROBLEM AND A STEP-BY-STEP CONSTRUCTION

Widom's potential distribution theorem$^{(10)}$ states that the average

$$\langle \exp[-\beta\psi(\mathbf{r})]\rangle_{N-1} \equiv \int_V \cdots \int_V d\mathbf{r}_1 \cdots d\mathbf{r}_{N-1} \exp\{-\beta\psi(\mathbf{r})\} \tag{1}$$

where $\psi(\mathbf{r})$ is the difference in potential energy when a particle is added at point $\mathbf{r}$ and the remaining $N-1$ particles are in the configuration $(\mathbf{r}_1,\ldots,\mathbf{r}_{N-1})$, equals the density $\rho(\mathbf{r})$ divided by the activity λ at every (inverse) temperature β. For hard-core interactions the Boltzmann factor $\exp\{-\beta\psi(\mathbf{r})\}$ can only take two values, 0 and 1, and therefore the average in Eq. (1) represents the probability $P(\mathbf{r})$ of finding enough free space around $\mathbf{r}$ to place a hard-core particle centered there. This probability depends, of course, on the size (and form) of the hard core, on the external potential, and on β and λ. We can use Widom's formula to determine the equilibrium $\rho(\mathbf{r})$ by considering first the inverse problem of constructing

$P(\mathbf{r})$ given $\rho(\mathbf{r})$ as the initial information, that is, finding a procedure of transforming the probability of finding a particle at $\mathbf{r}$ into the probability of finding a space for a particle at $\mathbf{r}$. Formally, this is accomplished by means of an (insertion) operator $\mathbf{q}$ such that $\mathbf{q}\rho(\mathbf{r}) = P(\mathbf{r}; \rho(\mathbf{r}))$. In this language Widom's theorem becomes an eigenvalue problem,(9)

$$\mathbf{q}\rho(\mathbf{r}) = \lambda^{-1}\rho(\mathbf{r}) \tag{2}$$

Thus, the first task is to determine $P(\mathbf{r}; \rho(\mathbf{r}))$ for a given hard-core interaction and external potential, and then having made Eq. (2) explicit, find the eigenfunctions $\rho(\mathbf{r})$ for every eigenvalue λ^{-1}. As we shall see, $P(\mathbf{r}; \rho(\mathbf{r}))$ turns out to be a nonlinear (and nonlocal) functional of $\rho(\mathbf{r})$, so that we obtain a framework similar to that of the BGYB and WLMB equations to search for solidlike oscillatory density solutions. Provided no approximations are introduced, Eq. (2) is equivalent to the other two, but in order to transform it into them, it is necessary to express $P(\mathbf{r}; \rho(\mathbf{r}))$ in terms of pair correlation functions. For our present purposes we do not need to consider pair correlations, nor any approximation regarding them. When the system is in a uniform state the probability of encountering spaces for addition of particles at density ρ, $P(\rho)$, is independent of $\mathbf{r}$. We define the uniform close-packing density ρ_{ucp} as that density for which $P(\rho) = 0$, and, according to Widom's formula, $P(\rho) = \lambda^{-1}\rho$, $P = 0$ is a state of infinite activity.

We consider now as a specific model system a lattice gas on a Bethe lattice with coordination number z (z can be arbitrary, but we present in this section detailed results only for $z = 3$, although in the following section we also include some numerical results for $z = 4$). Only the interior of a large lattice is studied and no reference is made to its boundary points. Particles occupy sites and exclude occupancy of other sites around them up to a fixed number of nearest neighbors k. In order to make reference to the position of any lattice site $\mathbf{s}'$ with respect to that of any other site $\mathbf{s}$, we introduce the following notation. Given a site $\mathbf{s}$, the z points around it form its first shell; further shells 2, 3,..., n around it are formed by connecting $z - 1$ points to each point in the previous shell. A point $\mathbf{s}'$ located j shells away from $\mathbf{s}$ is denoted by $\mathbf{s}' = \mathbf{s} + a_1 \cdot a_2 \cdots a_j$, where the sequence of numbers $a_1 \cdot a_2 \cdots a_j$ determines the path with no returns that connects site $\mathbf{s}$ to site $\mathbf{s}'$. In this sequence a_1 takes a value from 1 to z (and selects a point in the first shell), and a_2 to a_j take values from 1 to $z - 1$ (and each selects one point in each shell).

Nearest-Neighbor Exclusion Problem on the $z = 3$ Lattice. To solve this problem we need to find the probability $P(\mathbf{s}; \rho(\mathbf{s})) = n(\mathbf{s}, \mathbf{s}+1, \mathbf{s}+2, \mathbf{s}+3)$ that the four sites $\mathbf{s}$, $\mathbf{s}+1$, $\mathbf{s}+2$, and $\mathbf{s}+3$ are unoccupied when the probability for finding a particle at s is $\rho(\mathrm{s})$. Given the range of the interaction, and noticing that the removal of any bond in the lattice that connects nearest-neighbor sites breaks the lattice into two separate pieces, we have the following factorization:

$$n(\mathrm{s}, \mathrm{s}+1, \mathrm{s}+2, \mathrm{s}+3) = n(\mathrm{s}) \left[\frac{n(\mathrm{s}, \mathrm{s}+1)}{n(\mathrm{s})}\right]\left[\frac{n(\mathrm{s}, \mathrm{s}+2)}{n(\mathrm{s})}\right]\left[\frac{n(\mathrm{s}, \mathrm{s}+3)}{n(\mathrm{s})}\right] \tag{3}$$

where the functions in the rhs of Eq. (3) represent probabilities of finding the sites referred to in their arguments empty. The range of the interaction also implies that

$$m(\mathrm{s}, \mathrm{s}+a_1) = \rho(\mathrm{s}) \tag{4}$$

where $m(\mathrm{s}, \mathrm{s}+a_1)$ is the probability that a particle occupies site s and site $\mathrm{s}+a_1$ remains empty. In all cases the following relations hold:

$$n(\mathrm{s}, \mathrm{s}+a_1) + m(\mathrm{s}, \mathrm{s}+a_1) = n(\mathrm{s}+a_1) \qquad \text{and} \qquad n(\mathrm{s}) = 1-\rho(\mathrm{s}) \tag{5}$$

With the employment of Eqs. (4) and (5) in Eq. (3), Widom's formula in Eq. (2) becomes

$$\lambda^{-1}\rho(\mathrm{s}) = \frac{[1-\rho(\mathrm{s})-\rho(\mathrm{s}+1)][1-\rho(\mathrm{s})-\rho(\mathrm{s}+2)][1-\rho(\mathrm{s})-\rho(\mathrm{s}+3)]}{[1-\rho(\mathrm{s})]^2} \tag{6}$$

Next-Nearest-Neighbor Exclusion Problem on the $z=3$ Lattice. By following a procedure analogous to that described for the nearest-neighbor problem, we obtain

$$\begin{aligned}\lambda^{-1}\rho(\mathrm{s}) &= n(\mathrm{s}, \mathrm{s}+1, \mathrm{s}+2, \mathrm{s}+3)\\ &\quad\times\left[\frac{n((\mathrm{s}+1), (\mathrm{s}+1)+1, (\mathrm{s}+1)+2, (\mathrm{s}+1)+3)}{n(\mathrm{s}, \mathrm{s}+1)}\right]\\ &\quad\times\frac{n((\mathrm{s}+2), (\mathrm{s}+2)+1, (\mathrm{s}+2)+2, (\mathrm{s}+2)+3)}{n(\mathrm{s}, \mathrm{s}+2)}\\ &\quad\times\frac{n((\mathrm{s}+3), (\mathrm{s}+3)+1, (\mathrm{s}+3)+2, (\mathrm{s}+3)+3)}{n(\mathrm{s}, \mathrm{s}+3)}\end{aligned} \tag{7}$$

where the functions $n(\mathrm{s}, \mathrm{s}+1, \mathrm{s}+2, \mathrm{s}+3)$ and $n(\mathrm{s}, \mathrm{s}+1)$ have the same meaning as before and are given by

$$n(\mathrm{s}, \mathrm{s}+1, \mathrm{s}+2, \mathrm{s}+3) = 1-\rho(\mathrm{s})-\rho(\mathrm{s}+1)-\rho(\mathrm{s}+2)-\rho(\mathrm{s}+3) \tag{8a}$$

and

$$n(\mathrm{s}, \mathrm{s}+1) = 1-\rho(\mathrm{s})-\rho(\mathrm{s}+1) \tag{8b}$$

kth Nearest-Neighbor Exclusion Problem on the $z=3$ Lattice. Widom's formula for higher-order neighbor exclusion leads to forms similar to those in Eqs. (6) and (7), and $\lambda^{-1}\rho(\mathbf{s})$ is in these cases given by a larger number of factors, each of which is a ratio of probabilities for unoccupied sets of contiguous sites. In Fig. 1 we show these sets for various cases, the sites enveloped by the dashed lines represent a set involved in the probabilities that appear in the numerators of these factors, i.e., as in Eq. (8a), whereas the sites joined by the heavy lines represent a set involved in the probabilities in the denominators of these factors, i.e., as in Eq. (8b). A general expression for Widom's formula when k is odd can be written as

$$\begin{aligned}\ln[\lambda^{-1}\rho(\mathbf{s})] &\\ &= \ln[1-t(\mathbf{s})]\\ &\quad+\sum_{j=0}^{[k+1)/2}\ \sum_{a_1\cdots a_j}\ \sum_{b_1}\ln\left[1-\frac{\left(\begin{array}{c}\sum_{b_2\cdots b_{(k+1)/2}} n((\mathbf{s}+a_1\cdot a_2\cdots a_j)\\ +b_1\cdot b_2\cdots b_{(k+1)/2}))\end{array}\right)}{1-t(\mathbf{s}+a_1\cdot a_2\cdots a_j)}\right] \qquad (9)\end{aligned}$$

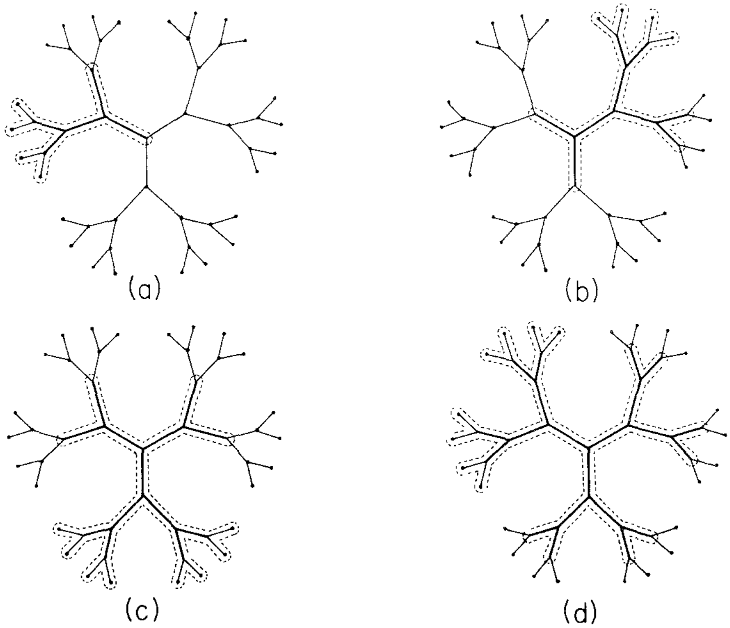

Fig. 1. Sets of contiguous sites whose probabilities for being unoccupied appear in Widom's formulas. The dashed lines enclose the points that appear in the numerators and the heavy lines join the points that appear in the denominators for the expressions for $\lambda^{-1}\rho(\mathbf{s})$. See the text. Depictions correspond to (a) fourth, (b) fifth, (c) sixth, and (d) seventh nearest-neighbor exclusions.

where

$$t(\mathbf{s}) = \sum_{j=0}^{(k+1)/2} \sum_{c_1 \cdots c_j} n(\mathbf{s} + c_1 \cdot c_2 \cdots c_j) \tag{10}$$

The summations in Eqs. (9) and (10) transform into integrations when the number of excluded shells of neighbors k goes to infinity while the lattice spacing is made to vanish. In deriving Eqs. (6), (7), and (9) we made no reference to the external field $v(\mathbf{s})$. When $v(\mathbf{s})$ differs from zero, λ in these equations is given by $\lambda = \exp\{-\beta[\mu - v(\mathbf{s})]\}$, where μ is the chemical potential.

3. BIFURCATION POINTS AND ORDER–DISORDER TRANSITIONS

It is now straightforward to obtain the thermodynamic behavior of the hard-core lattice gases considered in the previous section.

Nearest-Neighbor Problem. The equation of state for the liquid phase is obtained by considering the trivial solution $\rho(\mathbf{s}) = \rho$ in Eq. (6). This is

$$\lambda^{-1}\rho = \frac{(1-2\rho)^3}{(1-\rho)^2} \tag{11}$$

and, as would be expected, the uniform close-packing density is $\rho_{\mathrm{ucp}} = 1/2$. We subdivide the Bethe lattice into two interwoven sublattices such that every site in one sublattice has as nearest neighbor sites from the other sublattice. Equation (6) accepts different sublattice occupation numbers ρ_1 and ρ_2 provided

$$\lambda^{-1}\rho_1 = \frac{(1-\rho_1-\rho_2)^3}{(1-\rho_1)^2} \quad \text{and} \quad \lambda^{-1}\rho_2 = \frac{(1-\rho_1-\rho_2)^3}{(1-\rho_2)^2} \tag{12}$$

or

$$\rho_1(1-\rho_1)^2 = \rho_2(1-\rho_2)^2 \tag{13}$$

According to Eq. (13), the sublattice-ordered solution originates from the trivial uniform solution at a bifurcation point located at $\rho = 1/3$ and $\lambda = 4$. Away from this point the oscillatory solution develops amplitude (occupation builds up in one sublattice while the other becomes gradually empty) and increases monotonically in mean density and activity until it reaches close packing, $\rho_1 = 1$ and $\rho_2 = 0$ (or alternatively $\rho_1 = 0$ and $\rho_2 = 1$) and λ diverges. See Fig. 2a. A free energy analysis indicates that the bifurcation

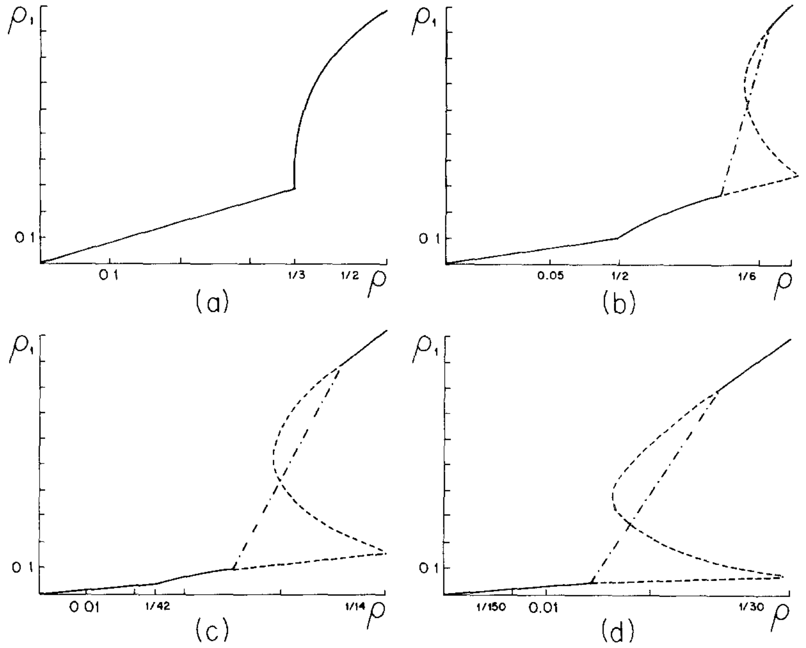

Fig. 2. Sublattice occupation vs. mean density for (a) first, (b) third, (c) fifth, and (d) seventh nearest-neighbor exclusions, respectively. The full lines represent equilibrium states and the dashed-dotted lines the join states where the first-order transition occurs. The number densities 1/3, 1/2, 1/42, and 1/150 correspond to those values for the second-order transitions, whereas 1/2, 1/6, 1/14, and 1/30 are the close-packing densities.

point is indeed a point of instability (the free energy curvature vanishes) and that the uniform liquid beyond this density and up to $\rho_{\text{ucp}} = 1/2$ is unstable (the free energy curvature is negative). Thus, we obtain a continuous order–disorder transition in analogy with the behavior found in the nearest-neighbor exclusion problem in the square, triangular, and honeycomb regular lattices.(12),[4] Here there is only one instability occurring before close packing, but, as we see below, this situation changes when the range of the interaction extends beyond the nearest neighbors.

Next-Nearest-Neighbor Problem. The equation of state for the liquid phase is obtained by considering the trivial solution $\rho(\mathrm{s}) = \rho$ in Eqs. (7) and (8). This is

$$\lambda^{-1}\rho = \frac{(1-4\rho)^4}{(1-2\rho)^3} \tag{14}$$

---

[4] See ref. 13 for the exact solution on the triangular lattice.

and indicates a uniform close-packing density $\rho_{\text{ucp}} = 1/4$. In this case we introduce four interwoven sublattices such that each point in one sublattice has as nearest-neighbors one point belonging to each of the remaining three sublattices. We are interested in sublattice-ordered solutions in which three sublattices have the same occupation number ρ_0 and the fourth sublattice has a different density ρ_1. Under this condition Eqs. (7) and (8) become

$$\lambda^{-1}\rho_1 = \frac{(1-\rho_1-3\rho_0)^4}{(1-\rho_1-\rho_0)^3} \quad \text{and} \quad \lambda^{-1}\rho_0 = \frac{(1-\rho_1-3\rho_0)^4}{(1-\rho_1-\rho_0)(1-2\rho_0)} \tag{15}$$

or

$$\rho_1(1-\rho_1-\rho_0)^2 = \rho_0(1-2\rho_0)^2 \tag{16}$$

According to Eq. (16), the sublattice-ordered solution originates now from the trivial uniform solution at a bifurcation point located at uniform close packing $\rho_{\text{ucp}} = 1/4$. This time the mean density decreases, and the activity λ becomes finite, when the oscillatory solution develops amplitude as it moves away from the branch point. See Fig. 3a. The grand potential for the

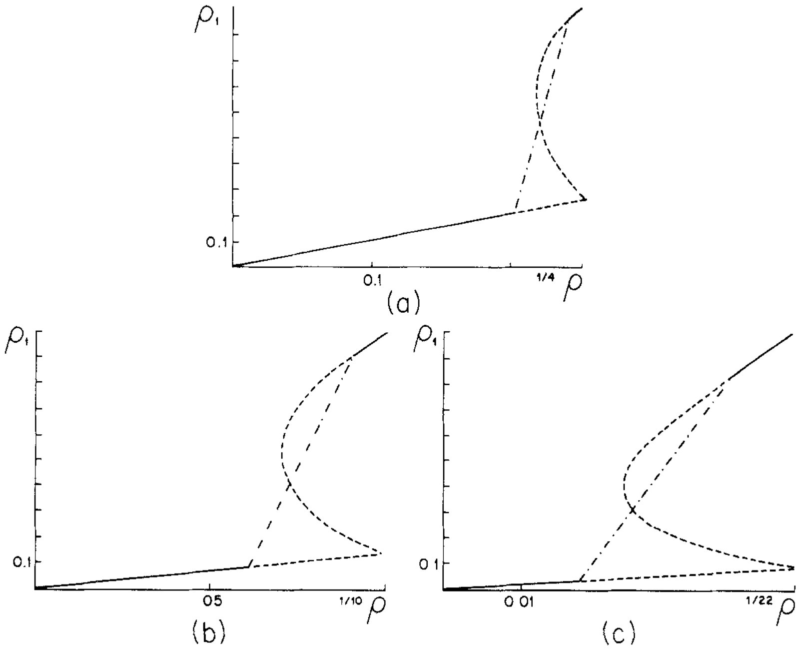

Fig. 3. Sublattice occupation vs. mean density for (a) second, (b) fourth, and (c) sixth nearest-neighbor exclusions, respectively. The full lines represent equilibrium states and the dashed-dotted lines the join states where the first-order transition occurs. The number densities 1/4, 1/10, and 1/22 correspond to the close-packing densities.

lattice gas ω (per four-site cluster, one of each sublattice) along the oscillatory solution is obtained by integration of Eqs. (15). This is

$$\omega = f - \mu(\rho_1 + 3\rho_0) \tag{17a}$$

where

$$\beta f = 4(1-\rho_1-3\rho_0)\ln(1-\rho_1-3\rho_0) + 3\rho_0 \ln \rho_0 + \rho_1 \ln \rho_1 \\ -3(1-\rho_1-\rho_0)\ln(1-\rho_1-\rho_0) - 3(1-2\rho_0)\ln(1-2\rho_0) \tag{17b}$$

and where f is the Helmholtz free energy (per four-site cluster). The pressure p can be obtained by substitution of Eqs. (15) into Eqs. (17) [with $\lambda = \exp(\beta\mu)$]. This is

$$\beta p = -\frac{1}{4} \ln \frac{(1-\rho_1-3\rho_0)^4}{(1-\rho_1-\rho_0)^3\,(1-2\rho_0)^3} \tag{18}$$

The free energy branch for the oscillatory solution can be analyzed and compared with the branch for the uniform solution $\rho_1 = \rho_0$. In Fig. 4 we show our results in βp vs. $\beta\mu$ space. We find a first-order phase transition at $\beta p = 3.559$ and $\beta\mu = 3.527$. There, the liquidlike solution has density $\rho_l = 0.203$ and the solidlike solution has sublattice densities $\rho_1 = 0.9602$ and $\rho_0 = 0.0014$, which imply a mean density $\rho_s = (\rho_1 + 3\rho_0)/4 = 0.241$; there-

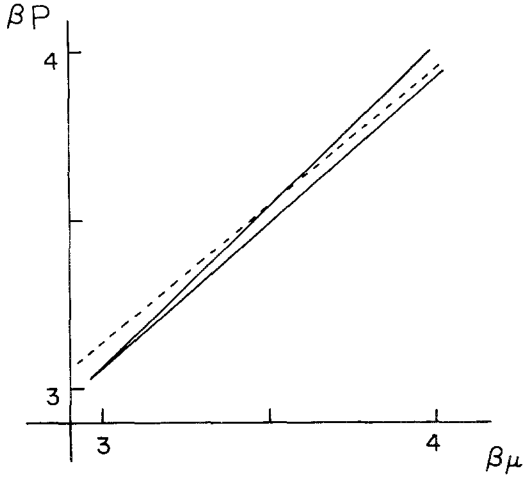

Fig. 4. Pressure vs. chemical potential plot for the uniform (dashed line) and sublattice-ordered (solid line) solutions of the next-nearest-neighbor problem. The solidlike solution originates from the liquidlike solution at a bifurcation point located at infinite p and μ. As observed, there is a sharp reversal in the solidlike solution, so that there are three lines extending to infinite p and μ.

fore the change in density at the order–disorder transition is about 16%. Our finding of a first-order transition in the next-nearest neighbor problem is analogous to that found via numerical calculations(14) for extended hard-core interactions in two-dimensional regular lattices when there is a uniquely defined sublattice-ordered close-packing arrangement.(15)

In Fig. 5b we show the results for the next-nearest-neighbor exclusion problem for $z = 4$; these can be compared with those for $z = 3$, also shown in Fig. 5a. It is interesting to note that the uniform fluid branch for this problem on the Bethe lattice is metastable between the first-order transition density and uniform close packing. That is, it can be analytically continued at the transition point.

Higher-Order Neighbor Exclusion Problems. In Figs. 2 and 3 we also show results for larger hard-core exclusion problems with $z = 3$. Those

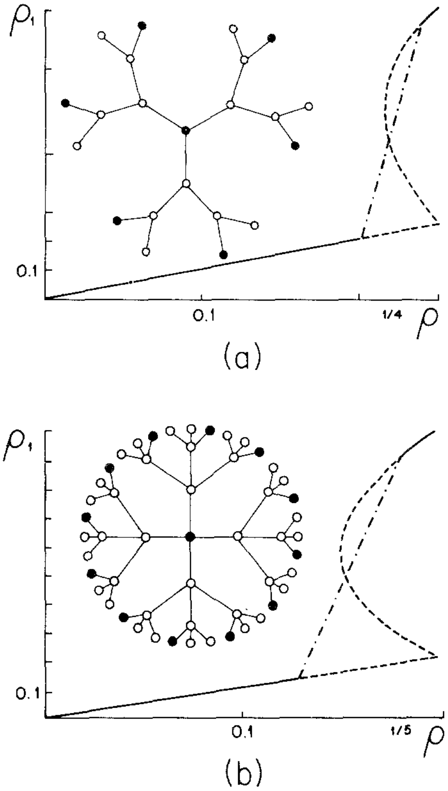

(a)

(b)

Fig. 5. Sublattice occupation vs. mean density for the next-nearest-neighbor exclusion problem, (*a*) $z = 3$ and (*b*) $z = 4$. The drawings illustrate close packing, with black circles indicating occupied sites.

in Figs. 2b, 2c, and 2d correspond, respectively, to up to third, fifth, and seventh nearest-neighbor exclusion, whereas those in Figs. 3b and 3c correspond, respectively, to up to fourth and sixth nearest-neighbor exclusion. For *odd* exclusion there are two bifurcations; the first occurs before close packing where the uniform solution gives way to a sublattice-modulated phase (with half-period equal to the lattice site spacing). This is a second-order transition. The second bifurcation takes place at close packing and here a third solution (in which all but one sublattice occupations are equal and one sublattice becomes eventually fully occupied while the others get empty) originates from the sublattice-modulated phase. In all cases we determined a first-order transition between the second and third solutions. For *even* exclusion there are only two solutions linked by a first order associated to only one bifurcation occurring at close packing, as is the case of the next-nearest-neighbor problem.

4. THE DIRECT CORRELATION FUNCTION AND APPROXIMATE THEORIES OF FREEZING

As mentioned above, existing theories of freezing$^{(1)}$ generally assume that the direct correlation function in the solid can be approximated by that of the uniform fluid. The hard-core problems we have analyzed here in the Bethe lattice provide an opportunity to assess this type of approximation, since both the nonuniform and uniform direct correlation functions can be known exactly. Here we present results for next-nearest-neighbor exclusion only. Functional differentiation of Eq. (7) leads to the following expressions for the direct correlation function:

$$c^{11}(0)=\frac{3}{1-\rho_1-\rho_0}-\frac{4}{1-\rho_1-3\rho_0} \tag{19a}$$

$$c^{00}(0)=\frac{2}{1-2\rho_0}+\frac{1}{1-\rho_1-\rho_0}-\frac{4}{1-\rho_1-3\rho_0} \tag{19b}$$

$$c^{10}(1)=\frac{1}{1-\rho_1-\rho_0}-\frac{2}{1-\rho_1-3\rho_0} \tag{19c}$$

$$c^{00}(1)=\frac{1}{1-2\rho_0}-\frac{2}{1-\rho_1-3\rho_0} \tag{19d}$$

and

$$c^{10}(2)=c^{00}(2)=-\frac{1}{1-\rho_1-3\rho_0} \tag{19e}$$

where the superindices and subindices correspond to the sublattice subdivision employed in Eqs. (15)–(18), and the arguments for the correlation 0, 1, and 2 indicate, respectively, same site, nearest-neighbor sites, and next-nearest-neighbor sites. The form of the direct correlation function for the uniform solution is obtained by setting $\rho = \rho_1 = \rho_0$ in Eqs. (19).

The grand potential functional Ω for the nonuniform lattice gas can be written as

$$\beta\Omega[\rho(\mathbf{s})] = \sum_{\mathbf{s}} \{\rho(\mathbf{s})[\ln \rho(\mathbf{s}) - 1] - \varphi(\rho(\mathbf{s})) - \beta\mu\rho(\mathbf{s})\} \tag{20}$$

where $\varphi(\rho(\mathbf{s}))$ is the difference in free energy between the ideal lattice gas and that under consideration. $\varphi(\rho(\mathbf{s}))$ can be approximated as

$$\begin{aligned}\varphi(\rho(\mathbf{s})) \approx \varphi(\rho) &+ \sum_{\mathbf{s}} \left.\frac{\partial\varphi}{\partial\rho(\mathbf{s})}\right|_{\rho} [\rho(\mathbf{s}) - \rho] \\ &+ \frac{1}{2}\sum_{\mathbf{s}}\sum_{\mathbf{s}'} c(\mathbf{s}, \mathbf{s}'; \rho)[\rho(\mathbf{s}) - \rho][\rho(\mathbf{s}') - \rho]\end{aligned} \tag{21}$$

where $c(\mathbf{s}, \mathbf{s}'; \rho)$ is the uniform fluid direct correlation function. It is straightforward to solve for the uniform and the sublattice-ordered solutions for the next-nearest-neighbor problem associated to the grand potential functional Ω in Eq. (20). We obtain for the densities at the transition $\rho_l = 0.2248$ and $\rho_s = (\rho_1 + 3\rho_0)/4 = 0.2288$, where $\rho_1 = 0.7039$ and $\rho_0 = 0.0704$. These values can be compared with the exact results given below Eq. (18). The change in density at the transition is now only 1.6%, an order of magnitude smaller than the 16% found for the exact solution (and which is similar to that observed experimentally in real substances). Also, the degree of sublattice ordering at the transition, $\rho_1 - \rho_0$, turns out to be 0.634, too small compared with that for the exact solution, which is 0.959.

ACKNOWLEDGMENTS

We are grateful to Prof. J. K. Percus for his guidance and encouragement in this problem. This work was supported partially by DGAPA-UNAM under contract IN-104189 and by CONACyT under contracts D111-903665 and D111-903655.

REFERENCES

1. M. Baus, *J. Stat. Phys.* **48**:1129 (1987); and A. D. J. Haymet, *Annu. Rev. Phys. Chem.* **38**:89 (1987).
2. R. Lovett, *J. Chem. Phys.* **88**:7739 (1988).
3. R. Lovett, C. Y. Mou, and F. P. Buff, *J. Chem. Phys.* **65**:570 (1976).
4. M. S. Wertheim, *J. Chem. Phys.* **65**:2377 (1976).

5. H. J. Raveché and C. A. Stuart, *J. Chem. Phys.* **63**:1099 (1975); **65**:2305 (1976).
6. H. J. Raveché and R. F. Kayser, *J. Chem. Phys.* **68**:3632 (1978); R. F. Kayser and H. J. Raveché, *Phys. Rev. B* **22**:424 (1980).
7. J. D. Weeks, S. A. Rice, and J. J. Kozak, *J. Chem. Phys.* **52**:2416 (1969).
8. R. Lovett, *J. Chem. Phys.* **66**:1225 (1977).
9. A. Robledo, *J. Chem. Phys.* **72**:1701 (1980).
10. B. Widom, *J. Stat. Phys.* **19**:563 (1978).
11. J. K. Percus, *J. Stat. Phys.* **15**:505 (1976).
12. D. S. Gaunt and M. E. Fisher, *J. Chem. Phys.* **43**:2840 (1965); L. K. Runnels and L. L. Combs, *J. Chem. Phys.* **45**:2482 (1966); L. K. Runnels, L. L. Combs, and J. P. Salvant, *J. Chem. Phys.* **47**:4015 (1967).
13. R. J. Baxter, *J. Phys. A* **13**:L61 (1980).
14. A. Bellemans and R. K. Nigam, *J. Chem. Phys.* **46**:2922 (1967); J. Orban and A. Bellemans, *J. Chem. Phys.* **49**:363 (1968).
15. R. M. Nisbet and I. E. Farquhar, *Physica* **73**:351 (1974).